Mechanism of surface modification on monocrystalline silicon during diamond polishing at nanometric scale

Prabhat Ranjan [1,2*], Tribeni Roy [3,4], Anuj Sharma [3]

[1]Bhabha Atomic Research Centre Mumbai, India, 400085
[2]Homi Bhabha National Institute Mumbai, India, 400094
[3]Department of Mechanical Engineering, BITS Pilani, India, 333031
[4]School of Engineering, London South Bank University, 103 Borough Road, London SE1 0AA, UK
* Corresponding author email address: pranjan@barc.gov.in

Abstract:

Demand of polished silicon wafer has increased significantly in the recent years to cater the development of the semiconductor industry. For example, polished silicon wafer has direct applications in integrated circuits, radio frequency amplifiers, micro-processors, micro-electromechanical systems, etc. To carry out mechanical polishing, lapping, grinding or single point diamond turning of silicon, diamond abrasive has been used extensively before implementation of chemo-mechanical polishing. During the diamond based polishing, few problems have already been identified such as formation of amorphous phase, heat affected zones, low material removal, etc. Some research works have also reported that nano-structured abrasive leads to thin layer of the amorphous phase and better material removal rate. In the same direction, a molecular dynamics simulation is carried out in this paper to investigate the mechanism of material removal from monocrystalline silicon during the diamond abrasive based polishing process. The present work is mainly focused on the dynamics of material removal phenomenon near the abrasive particles at nanometric scale by considering stress, lattice, cohesive energy, etc. This reveals that higher value of indentation force results in the surface buckling which creates a zone of both compressive as well as tensile stresses, which increases coordination number and forms β-silicon just ahead of abrasive particle. This mechanism happens by developing β-silicon phase on the surface with thickness beyond a certain value of indentation force on the zone of compression. Buckling on this phase happens due to stress localisation in compression as the flow stress of this phase is lesser than diamond cubic lattices. To avoid the mechanism of surface buckling and process silicon material on the surface, the indentation force needs to be maintained below a critical value. In the present case, it was found that the indentation force less than or equal to 190 nN for the abrasive size of ϕ8nm does the material removal by surface processing only without surface buckling. It was also found that the surface processing helps to reduce the depth of amorphous layer significantly without compromising the material removal rate and without generation of wavy surface. Thus, the present mechanism will help in polishing of silicon with minimum defects and reducing processing time for final stage of polishing towards manufacturing ultra-smooth and planer surface.

Keywords: Molecular dynamics, LAMMPS, Polishing, Silicon, β-silicon, Surface buckling.

Introduction

In the present era of advanced technology for semiconductor industry, fabrication with high spatial resolution helps to build high density devices. To carry out such type of nanofabrication, silicon surface needs to be made with ultra-smooth surface in terms of high surface finish and planarization which is possible with the help of chemical mechanical polishing (CMP) process [1]. In the recent development of CMP towards ultra-precision polishing, various advancements are being carried out. For example, environment friendly additives have been investigated such as sorbitol, gluconic acid, citric acid, and ammonium citrate within the polishing slurry for better material removal rate [2]. Furthermore, potassium ions have been employed in the polishing slurry to improve the material removal rate by 53.42 % under the presence of monodisperse alkaline colloidal silica, organic/inorganic acids and inorganic salts [3]. The development in CMP technology has increased the usage and application of silicon for electronic devices, industrial automation, computer systems, and precision optics more frequently [4,5]. As far as processing of silicon material for nanofabrication is concerned, there are many technologies. But only few of them are used to build initial shape or platform for fabrication. These technologies are known as wire-EDM, mechanical polishing, diamond turning, chemo mechanical polishing etc. towards making silicon wafer. While processing silicon with these techniques, there is a great chance about the formation of subsurface damage and cracks when process parameters are not selected properly, and removal of these damages becomes difficult [6]. Yana et al. [7] have carried out molecular dynamics simulation to study the effect of the diamond tip orientation with scratching direction while nanomachining or scratching of monocrystalline silicon. It was reported that the change of the contact due to the tip orientation and scratching direction affects the scratching forces significantly. During scratching, the normal force was found more sensitive with respect to the tangential forces. The tip orientation also affects the plastic deformation of silicon material. As far as stress distribution is concerned, it is mainly related with the geometry of the diamond tip. This stress further introduces the phase transition zone. Thus, the tip orientation affects the distribution of induced amorphous silicon atoms. For example, larger tilt angle of the tip with face-based scratching directions leads to induce more amount of damage during the scratching. Another study was conducted by Nguyena and Fang to investigate the effect of sliding, rolling and oscillating motion of diamond abrasive particles to establish nanotribology properties of a diamond abrasive against a silicon substrate [8]. Various parameters were studied for material removal characteristics such as abrasive size, sliding velocity, depths of polishing, rolling velocity, rolling direction, oscillating amplitude and oscillating frequency. Based on this study, it was observed that the rolling mechanism leads to high material removal rate, whereas, the oscillating mechanism helps in reducing height of asperity and minimise it. Therefore, the oscillating motion of diamond abrasive has significant contribution for wiping out the asperity atoms from the surface of monocrystalline. However, the oscillating motion with high amplitude and a low frequency leads to surface defects on the flat surface of silicon. Ranjan et al. [9] reported the material removal mechanism on aluminium and silicon during mechanical polishing and it was observed that the nanometric polishing with diamond abrasives does abrasion with the mechanism of adhesion de-bonding in which silicon forms non-crystalline debris. When polishing of both materials were compared, it was found that the potential energy

of silicon increases tremendously which indicates to form highly unstable surface in terms of physical as well as chemical stability. Another study on the mechanical polishing of monocrystalline silicon shows the phase transformation occurs due to high temperature as well as excessive value of hydrostatic pressure, which further results the transformation of silicon microstructure from the diamond cubic to the six-coordinated body-centered tetragonal structure or β-silicon phase [10]. Zhu et al. [11] investigated ductile mode machining (which is brittle to ductile transition during machining) of monocrystalline silicon during diamond tool elliptical vibration-assisted nanocutting (EVANC) and traditional nanocutting process via molecular dynamic simulations. EVANC induces smaller zone of stress-affected region which leads a thinner phase transformation layer as compared with the traditional nanocutting. This helps to achieve better surface finish and higher material. In EVANC, the machining forces are relatively lower because of the change in the brittle to ductile transition which also helps to reduce the tool wear. Another study about the ductile cutting was carried out using a nanostructured diamond tool on a single crystal silicon through molecular dynamic simulations [12]. The material removal behavior was studied by considering the parameters of groove direction, depth, width, factor, etc. It was found that the groove orientation of 60 degree helps to reduce cutting force up to minimum value which results in decrease of the induced cutting heat more β-silicon phase, less von-Mises stress and hydrostatic stress. On other hand, smaller groove orientation, groove depth and groove width, and larger groove factor yield cutting through ductile mode with high material removal rate. The study of this work is somewhat similar with EVANC as the nanostructured tool does intermittent contact what EVANC does. For mechanical polishing, similar concept of the ductile mode machining was also implemented using nano-structured diamond abrasives on single-crystal silicon using molecular dynamics simulation [13]. Obviously, the analysis reports that the nano-structured abrasive helps to polish silicon with lower forces, thinner subsurface damage layer, lower hydrostatic stresses, lower defect atom numbers, and less compressive normal stresses. Effect of relative tool sharpness (RTS) which is directly related with the depth of uncut chip thickness, on subsurface damage and material recovery was studied using diamond tool based cutting of mono-crystalline silicon at molecular scale [14]. It was observed that higher RTS induces subsurface damage layer in serration form due to stick-slip phenomenon. Depth of the serration is directly related to the value of RTS without affecting its frequency. Progression of nano-cracks in single-crystal silicon is investigated during ultra-precision mechanical polishing at atomic scale [15]. It was noticed that initial cracks of a defective material get closed instead of its expansion during mechanical polishing process. The mechanism of the crack closure is due to the coordinated displacement of atoms followed by the phase transformation filling of atoms in the crack zones. After the crack closure, there is significant changes in the coordination number of silicon atoms. Moreover, it is also reported that this effect of the crack closure is achieved more efficiently at temperature of 600 K.

Based on the studies reported on diamond based polishing or machining, few problems have already been identified such as formation of amorphous phase, heat affected zones, low material removal, etc. Some research works have also reported that the intermittent contact between tool and workpiece helps to thin down the layer of the amorphous phase and efficient material removal [11–13]. However, there is a dearth of work reported for the mechanism of

surface and sub-surface damages, material removal and generation of defect-less surface during conventional polishing process of silicon. As far as experimental studies through atomic force microscope, electron microscope, X-ray photospectroscope, etc. are concerned, it is impossible to investigate the mechanism of any polishing process at pico-second, nano-second and nanometric scale. However, molecular dynamics simulation (MDS) with Tersoff pair-potential has already validated in literature [16,17]. Hence, a molecular dynamics simulation is carried out to investigate the mechanism of material removal from the monocrystalline silicon using diamond abrasive based polishing. In this paper, stress distribution and phase transformation are studied towards formulating the mechanism of material removal for polishing of silicon with minimum defects of ultra-precision manufacturing to improve understanding of material removal during, CMP, single point diamond turning, diamond grinding, lapping etc.

Molecular Dynamics Simulation

In this section, details of molecular dynamics simulation (MDS) are presented and discussed. Parameters of the simulation is shown in *Table 1*. During the simulation, few assumptions were used such as spherical shape of abrasive, flat workpiece, thermostat atoms for heat conduction within workpiece, damping force for fluid viscous force, periodic boundary conditions along X-axis and Y-axis, shrink boundary condition along Z-axis, and interaction zone without any other chemicals.

Table 1: Parameters of molecular dynamics simulation.

S.N.	Parameters	Value
1.	Workpiece material	Monocrystalline silicon with surface of (001) plane
2.	Fixed base of workpiece	27.2 nm x 10.9 nm x 0.54 nm
3.	Thermostat region of workpiece	A block of 27.2 nm x 10.9 nm x 3.0 nm
4.	Newtonian region of workpiece	A block of 27.2 nm x 10.9 nm x 7.3 nm
5.	Lattice structure of workpiece	Diamond cubic with Lattice constant =0.5432 nm
6.	Number of atoms on workpiece	1,62,000
7.	Abrasive particles	Mono-crystalline Diamond (C)
8.	Size of abrasive particle	ϕ8nm with 47337 atoms
9.	Lattice structure of abrasive	Diamond cubic (DC) with lattice constant =0.357 nm
10.	Polishing force	F_x=3.8 μN and F_z=95 nN to 757 nN
11.	Time step	0.25 fs
12.	Simulation time	56 ps
13.	Viscous damping on abrasive	$1.8x10^{-8}$ gm/s
14.	Boundary	X: periodic, Y: periodic, Z: shrink

The MDS model to carry out the polishing process on silicon workpiece is shown in *Fig.1* in which two type of forces are applied on the abrasive particle. Here, F_x belongs to the abrasion force along X-axis and F_z is the indentation force. This indention force is applied opposite to the Z-axis as shown in *Fig.1*. In general, polishing pressure for chemo-mechanical polishing becomes 30 kPa-0.2 MPa and the size of diamond abrasives are in order of sub-microns to few microns. Hence, Fz is calculated based on the diameter of diamond abrasive for 2 μm and pressure in the range of 30 kPa-0.2 MPa. Thus, effect of indentation force on polishing is aimed

by varying F_z (F_z is multiplication of polishing pressure and projected area of abrasive) with four different level of 95 nN, 190 nN, 379 nN and 757 nN. In the present molecular study work, abrasive size is taken very small to minimise the computation time. The smaller abrasive may lead to get lodged on the workpiece if Fx is not sufficiently high. Hence, Fx is kept at least one order higher than Fz and due to this Fx is set to 3.8 μN. When an abrasive particle movement is allowed to travel under specified forces then the abrasive particle rolls instead of sliding which is a pure imitation of a polishing process. In general, polishing through lapping or chemo-mechanical polishing, water is used as a polishing medium due to its excellent thermal conductivity and chemical attributes to interact with polishing materials. In view of this, the present work tries to simulate the effect of water medium on the entire system by imposing the thermal and damping attributes of water instead to direct modelling of water molecule as presented in *Table 1*. For temperature control, the thermostat atoms are maintained at 300K by assuming that ambient and polishing slurry temperature is at room temperature of 300K.

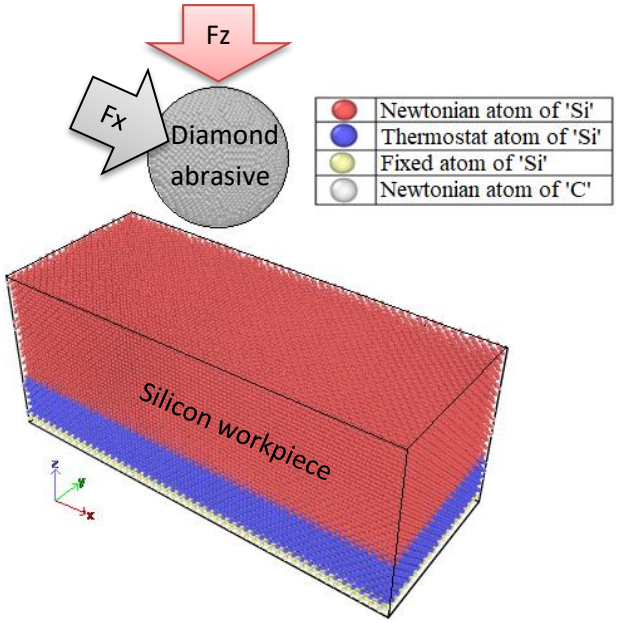

Fig. 1. MDS model for polishing of silicon using diamond abrasive.

Velocity and position of the Newtonian atoms of *Fig.1* are governed by Newton's second law of motion and fixed base atoms are frozen i.e. zero velocity. Velocity and position were calculated by the direct integration of the classical Hamiltonian equations of motion using the Velocity-Verlet algorithm. The polishing process was simulated under the statistical ensemble of constant micro-canonical ensemble (NVE) which consists of a constant number of atoms (N), the system's volume (V) and the total energy in the system (E) excluding the heat dissipation from the thermostat region of workpiece as the thermostat region is included to imitate the effect of heat conduction due to the presence of water.

To model and simulate diamond cubic of silicon and carbon, Tersoff potential is used on analytic bond-order potential (ABOP) derived interaction on Si-Si, C-C, and Si-C. The Tersoff potential has capability for 3-body interaction with attractive Morse potential, short range repulsive potential, bond-order, and bond angle information as expressed in Eq.1.

$$E = \frac{1}{2}\sum_{i>j} f_c(r_{ij})\left[V_R(r_{ij}) + b_{ij}V_A(r_{ij})\right] \quad (1)$$

Where 'E' is the Tersoff potential which is combination of pairwise repulsive (V_R) and attractive (V_A) contributions in an explicit manner to fit ABOP derived potential. 'fc' indicates the thermal vibration attributes of the potential well phenomenon. Thus, this potential exhibits repulsion force when gap between atoms becomes less than the equilibrium gap. In case of larger gap, attractive force dominates with respect to the orientation as modelled by b_{ij} in Eq.1.

$$V_R(r) = Ae^{(-\lambda_1 r)}; \quad V_A(r) = -Be^{(-\lambda_2 r)}; \quad b_{ij} = \left(1 + \beta^n \zeta_{ij}^n\right)^{-\frac{1}{2n}}; \quad \zeta_{ij} = \sum_{k(\neq i,j)} f_c(r_{ik})\, g(\theta_{ijk}) e^{[\lambda_3^m (r_{ij} - r_{ik})^m]};$$

$$g(\theta_{ijk}) = \lambda_{ijk}\left(1 + \frac{c_i^2}{d_i^2} - \frac{c_i^2}{d_i^2 + (\cos\theta_{ijk} - \cos\theta_0)^2}\right);$$

Where, i, j, and k are the atomic labels, r_{ij} is the bond length between the atoms i and j, and θ_{ijk} is the bond angle between the ij and ik bonds. 'b_{ij}' is known as bond order, and g(θ) is known as angular momentum. The cut off function (f_c) is defined as follows.

$$f_c(r) = \begin{cases} 1 & r < R + D \\ 0 & r > R + D \\ \frac{1}{2} - \frac{1}{2}\sin\left(\frac{\pi}{2}\frac{r - R}{D}\right) & |R - r| \le D \end{cases}$$

Where, 'R' and 'D' represent the position and the width of the cutoff region respectively.

The Tersoff potential parameters are listed in *Table 2*.

Table 2: Potential function parameters for Si-Si, C-C and Si-C interactions [16,17]. Where m, γ and λ_3 ($Å^{-1}$) were set constant with the value of 3, 1 and 0 respectively.

Pairs	c	d	Cosθ₀	n	beta	λ₂ (Å⁻¹)	B	R	D	λ₁ (Å⁻¹)	A
C-C-C	38049	4.3484	-0.57058	0.72751	1.57E-07	2.2119	346.7	1.95	0.15	3.4879	1393.6
Si-Si-Si	100390	16.217	-0.59825	0.78734	1.1E-06	1.73222	471.18	2.85	0.15	2.4799	1830.8
Si-Si-C	100390	16.217	-0.59825	0	0	0	0	2.36	0.15	0	0
Si-C-C	100390	16.217	-0.59825	0.78734	1.1E-06	1.97205	395.126	2.36	0.15	2.9839	1597.311
C-Si-Si	38049	4.3484	-0.57058	0.72751	1.57E-07	1.97205	395.126	2.36	0.15	2.9839	1597.311
C-Si-C	38049	4.3484	-0.57058	0	0	0	0	1.95	0.15	0	0
C-C-Si	38049	4.3484	-0.57058	0	0	0	0	2.36	0.15	0	0
Si-C-Si	100390	16.217	-0.59825	0	0	0	0	2.85	0.15	0	0

To ensure better accuracy of the result, smallest time step in the scale of femtosecond (fs) is recommended during MDS [18]. However, lesser time step also increases the computation effort. Hence, the time step of 0.25 fs was set for the present study. The abrasive particle was allowed to move under influence of an external force and viscous damping. In the present work, LAMMPS software [19] has been used to perform a series of simulations as per the *Table 1*. To visualize the result of the simulation, OVITO software [20] is used, and further analysis is performed using post processing on the output data of the simulation.

Equilibration of MDS Model

Before running the actual dynamics of simulation, it is better to equilibrate the entire model to optimise the position of all atoms. It helps to place all atoms in a well-defined equilibrium positions, and by this technique, cohesive energy of materials gets stabilized and becomes constant with time during MD simulation. In this work, equilibration was carried out in two stages. The first stage was used to obtain optimum lattice size of both abrasive as well as workpiece. In the second stage, velocity of all atoms except fixed atoms was set to the equivalent thermal atoms of 300 K. Subsequently, temperature was rescaled for every 5 steps of simulation under NVE ensemble up to 4000 steps or total time of 1 ps.

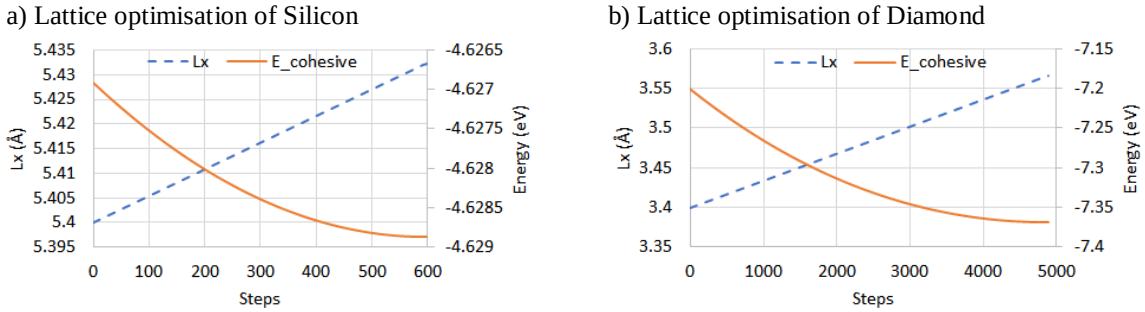

Fig.2: Lattice optimization with respect to cohesive energy (a) for Silicon and (b) diamond.

During the lattice optimisation, zero external pressure was applied to the lattice box by using the technique of energy minimization. This energy minimisation simulation was performed with the maximum change in volume of 0.001 % of the box under the conjugate gradient algorithm. It was observed that stress or pressure on the box becomes zero and cohesive energy gets minimised as shown in *Figs.2(a-b)*. This result yields the optimum lattice constant of 5.4321 Å on Silicon and 3.5658 Å on Diamond.

Furthermore, these lattice constants were used to build the MDS model for the second stage of equilibration to minimise cohesive energy for both abrasive particle and workpiece as presented in *Fig.3 (a-b)*. It is noticed that the cohesive energy of both gets quickly stabilizes with small fluctuation, and the reason might be due to the implementation of optimised lattice while building the model. The equilibrated condition has further been used for actual MD simulation and the same is presented in the next section of this paper.

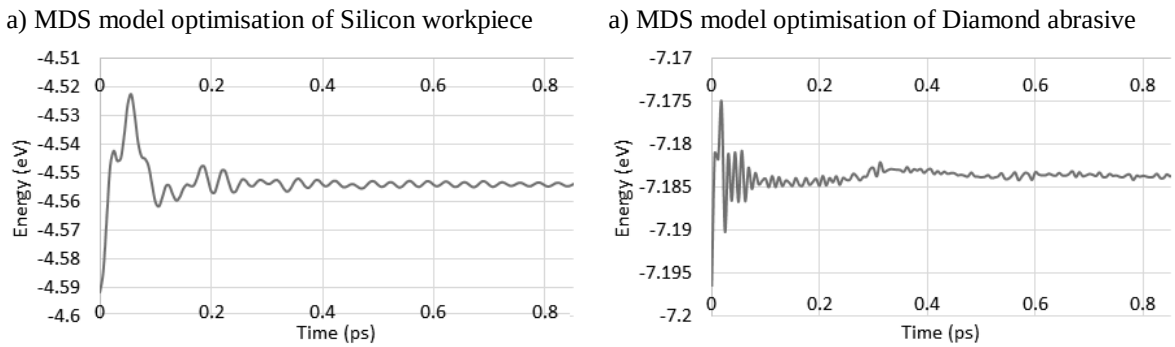

Fig.3: Variation of cohesive energy with time step for (a) workpiece, (b) abrasive particle

Methods of Analysis

Atomistic stress: Interaction between atoms of abrasive and workpiece leads to stresses for deforming material. In general, virial stress [21] is used to compute stress on individual atoms. From the analysis point of view, von-Mises stress [22] has also been computed which tells about equivalent stress on a specific atom instead of having a set of stress matrix.

Common neighbor analysis: Structure analysis is an essential aspect to characterize arrangement of atoms for discriminating diamond cubic (DC) and amorphous structures through adaptive common neighbor analysis method [20].

Coordination analysis: This technique is used to compute number of neighbor atoms corresponding to a specified atom provided they are within a given cutoff radius (r_c). This computed number is called as coordination number to the specific atom. This analysis is also extended to study about radial distribution function which describes how density varies as a function of distance from the specified atom, and it also characterizes the 'order degree' of a cluster of atoms in silicon workpiece as far as lattice information is concerned. This analysis tool is used to characterize phase transformation, if any in workpiece during the polishing process.

Radial distribution function (RDF): The radial distribution function (RDF) is an analysis tool which is typically used to illustrate the atom's 'order degree' of a specified domain. To evaluate the 'order degree' of the workpiece during the polishing, the calculation of RDF at different steps is carried out as per Eq.2.

$$g(r) = \frac{\rho_r(4\pi r^2)dr}{\rho_r^{id}(4\pi r^2)dr} \qquad (2)$$

Where, 'r' is radius of a spherical shell with thickness equal to 'dr'. 'dr' is comparable with atom diameter. 'ρ_r' and 'ρ_r^{id}' are number density of atoms in actual system and ideal gas respectively.

Results and discussions

Stress at atomistic level is analysed for Virial as well as von-Mises and the same are presented in *Figs.4(a-d)* for higher indentation force which is 757 nN. *Fig.4(a)* shows that there will be almost zero stress initially as the external force is not applied on workpiece. During indentation time, abrasive starts applying indentation up to the assigned value of F_z, e.g., 757 nN is this case. Due to this indentation, compressive stress builds along X-axis or lateral direction as shown in *Fig.4(b)*. Whereas, a combination of both tensile as well as compressive stresses induces along indentation or Z-axis as shown in *Fig.4(c)*. This type of tensile and compressive stresses build based on the type of deformation as shown there itself. When abrasive indents, workpiece atoms beneath the abrasive gets movement along X-axis and it tries to generate compression and due to this compressive stress builds. At the same instance, atoms also try to move from lower portion of abrasive to the surface of workpiece to minimise its own potential

energy, which further induces a pulling force nearby the bottom point of abrasive and a pattern of tensile and compressive stresses builds.

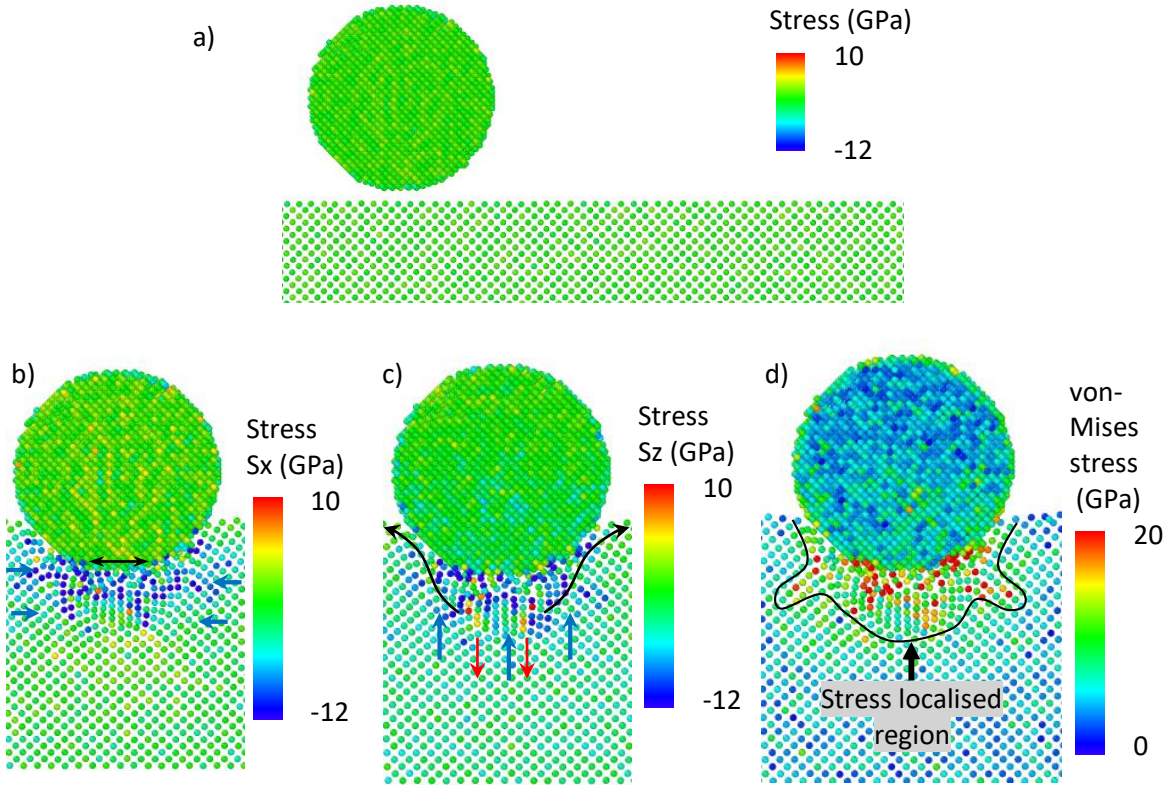

Fig.4: Atomistic stress during indentation with Fz=757 nN. (a) Virial atomistic stress before initial contact. (b) Virial stress along lateral direction during indentation. (c) Virial stress along indentation direction during indentation. (d) von-Mises stress during indentation.

When equivalent stress or von-Mises stress was evaluated to understand the zone of stressed region, it was observed that a typical shape is made which also indicates that the stress gets localised and it tries to spread along lateral direction instead of indentation as shown in *Fig.4(d)*.

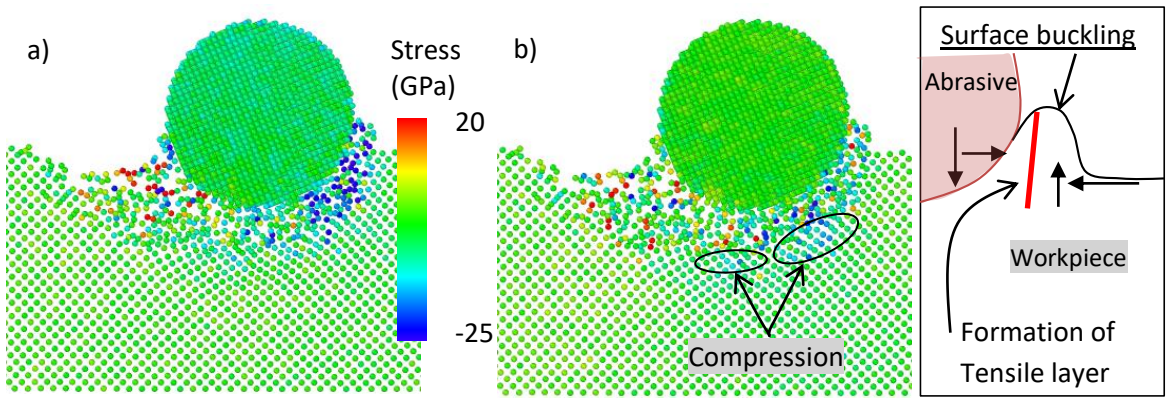

Fig.5: Atomistic Virial stress during polishing with Fz=757 nN. (a) Atomistic stress along lateral direction. (b) Atomistic stress along indentation direction with the mechanism of surface buckling.

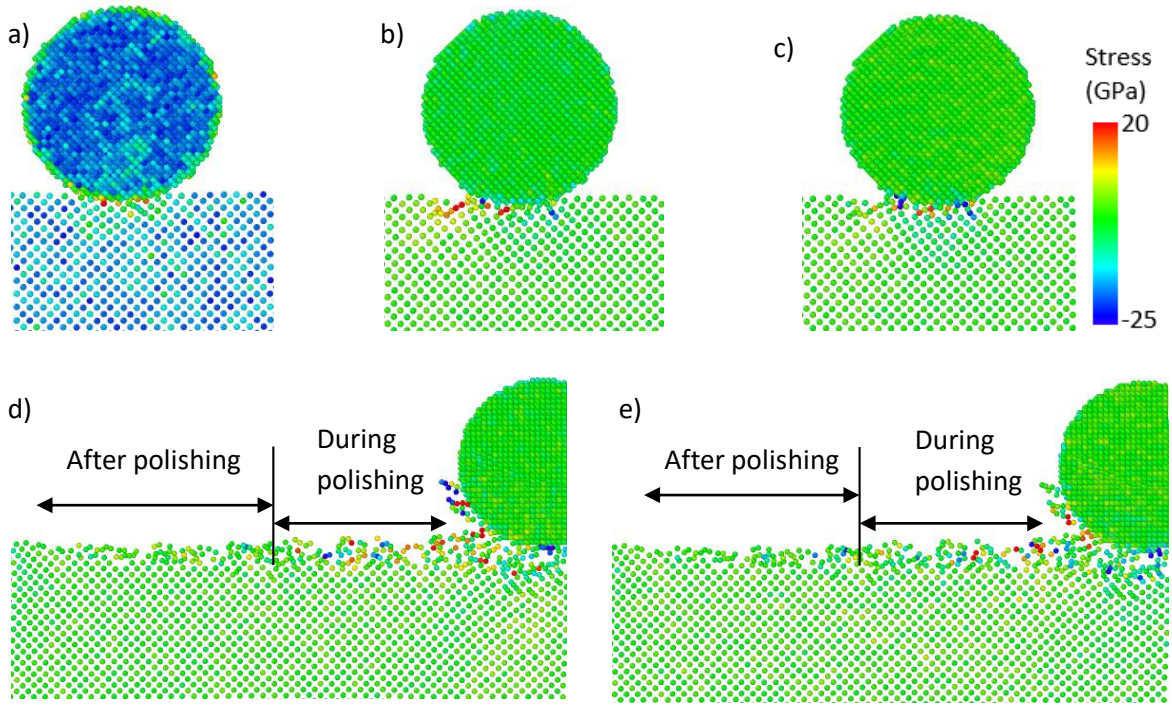

Fig.6: Atomistic stress during polishing with Fz=95 nN. (a) von-Mises stress during indentation. (b) Virial stress at the start of polishing along lateral direction. (c) Virial stress at the start of polishing along indentation direction. (d) Virial stress after polishing along lateral direction. (e) Virial stress after polishing along indentation direction.

During polishing process, the abrasive starts moving along lateral direction under the influence of F_x (which is kept equal to 3.8 μN to avoid abrasive loading on the workpiece) force. In this case, abrasive starts rolling due to the induction of rotating moment (M) based on F_x and the resistance force (F_m) form workpiece as shown in *Fig.5(a)*. Due to this rolling behaviour of motion, atoms of polished surface initially show tensile stress which tries to relax with time, and the Si-atoms ahead of abrasive experience compressive stress as shown in *Fig.5(a)*. To analyse furthermore, stress along indentation is also computed and presented as shown in *Fig.5(b)*. It also shows similar behaviour. Moreover, few atoms in front of abrasive also experience tensile stress along Z-axis due to the phenomenon of surface buckling. The mechanism of surface buckling inducing these tensile atoms as shown in an inset photo of *Fig.5(b)* which indicates that the surface of Si-atoms experiences compressive force along X-axis. This compressive force tries to buckle which get direction due to the resistance force from Si-workpiece along Z-axis and it further induces tensile stress on one or few atomic layer. The surface buckling is an unwanted phenomenon which will increase the required energy for material removal during polishing and it induces more defects on Si-workpiece.

In order to avoid the surface buckling effect, similar study for the stress analysis is carried out with lesser value of the indentation force of 95nN and the same is presented in *Figs.6(a-e)*. *Fig.6(a)* shows that there will be an attractive force followed by compression when abrasive approaches workpiece during indentation and it is limited up to the surface only. *Figs.6(b-c)* show that the trailing atoms to the abrasive experience pure tension, and leading atoms experience compression. The tensile stress is higher along X-axis and compression along Z-axis when *Figs.6(b&c)* are studied. These results do not show any indication about the surface buckling and due to this it can be treated as an efficient polishing technique. *Figs.6(d-e)* show

that tensile stress along X-axis is the key factor for the material removal as it is highest among other stresses along X and Z –axes. As polishing progresses, the polished surface show free from any kinds of residual stress in tension and compression.

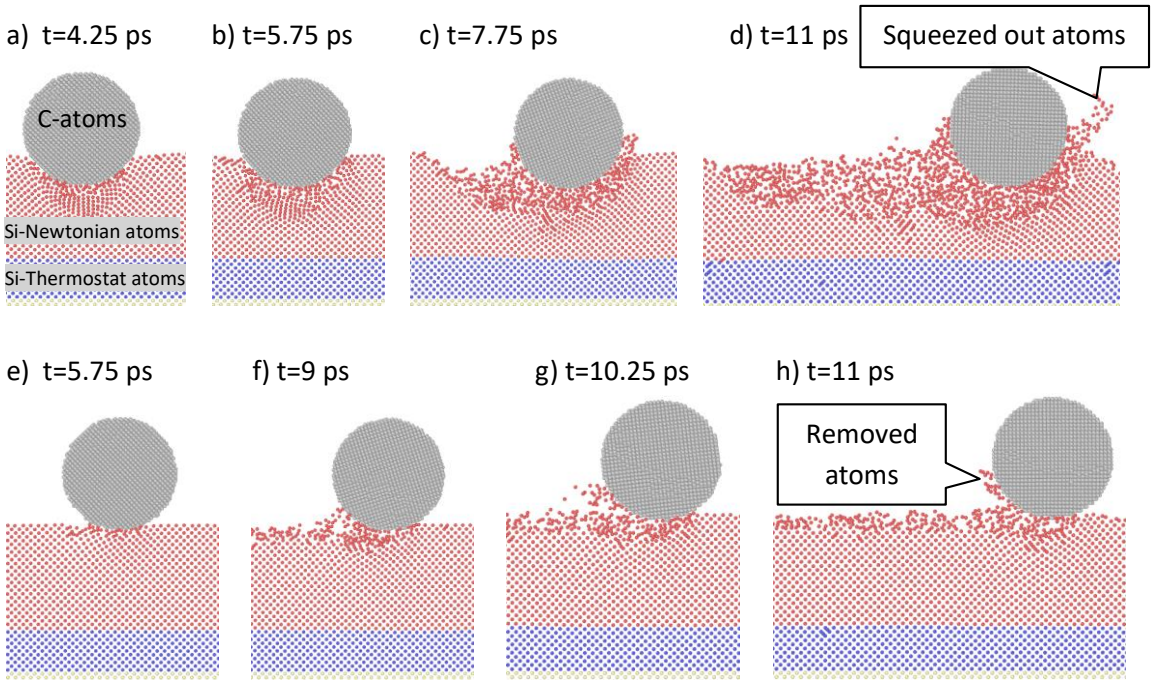

Fig.7: Atomic configurations of abrasive and workpiece atoms with different time of polishing. (a-d) with indentation force =757 nN. (e-h) with indentation force =95 nN.

Atomic configuration during polishing with different time is presented for both forces of 575 nN and 95 nN as shown in *Figs.7(a-h)*. *Fig.7(d)* shows the chip formation in form of squeezed film of Si-atoms due to the formation of surface buckling as shown in *Fig.7(c)*. In this case, material removal is taking place by both adhesion-debonding [9] and surface buckling. Here, the surface buckling induces more resistance to the abrasive which may also try to entrap the abrasive within the surface of Si-atoms. In case of smaller indentation force, material removal is taking place purely in form of rolling followed by adhesion debonding as shown in *Figs.7(e-h)*. Thus, the diamond polishing on silicon workpiece works in following two mechanisms.

- Polishing with surface buckling
- Polishing without surface buckling

In order to understand these two mechanisms on the phase transformation, lattice structures of workpiece was investigated through common neighbour analysis and coordination number analysis which are presented in *Figs.8 and 9*.

Figs.8(a-h) show the phase transformation at different time of polishing at 757 nN and 95 nN of indentation force. It is observed that while indentation, diamond cubic (which is coloured in blue) gets amorphous (in while colour) up to a certain depth which depends on the indentation force. This depth of amorphous layers gets maintained even after removal of abrasive. This might be happening due to the compression of the amorphous layers and irreversible phase

which are beneath the abrasive. When this study was carried out with different levels of indentation forces, it was found that the indentation force directly affects the depth of amorphous layer after polishing. Therefore, it is essential to polish Si-workpiece in stage wise manner in which indentation force (or polishing pressure in lapping or chemo-mechanical polishing) can be small for the last stage of polishing to minimise the surface defects towards ultra-precision polishing.

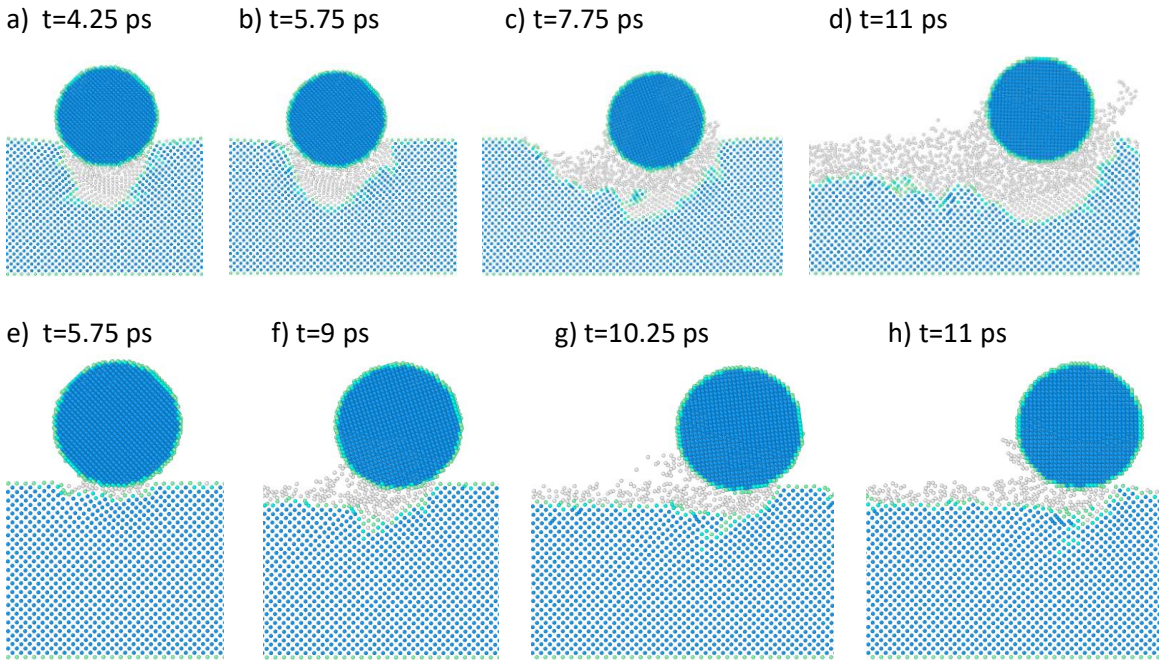

Fig.8: Lattice structure of workpiece atoms with different time of polishing. Blue colour indicates diamond cubic structure and while colour shows amorphous phase. (a-d) with indentation force =757 nN. (e-h) with indentation force =95 nN.

For further insight about the phase transformation, coordination number was also analysed by setting the cut-off radius of 3 Å and they are presented in *Figs.9(a-h)* in which coordination number 4 is hidden as it belongs to diamond cubic (or SP^3) structure. While analysing this results, it was found that it has similar behaviour with earlier results of phase transformation. Moreover, this study on coordination number gives more insight about the type of amorphous phase transformation. During the indentation process, coordination number (CN) 5 appears which is β-phase of silicon and it further turns in to CN 6 based on higher compressive force as shown in *Fig.9(a).* When *Fig.8(a)* and *Fig.9(a)* are compared, it is noticed that the CN 6 leads to the amorphous layers of Si and it remains constant in quantity. After progressing of polishing, the trailing atoms of abrasive shows few atoms of Si with coocrdinationnumber less than CN 4 which indicates debonding of Si-atoms from diamond cubic stricture in tension as shown in *Figs.9(c-d)* and *Figs.9(f-h)*. Thus, the lattice transformation silicon during diamond polishing obeys following two mechanisms.

- Transformation under compressive stress: CN 4 →CN 5 → CN 6 or diamond cubic Si →β-Si → amorphous Si.

- Transformation under tensile stress: CN 4 →CN 3+ CN2 or diamond cubic Si →amorphous Si.

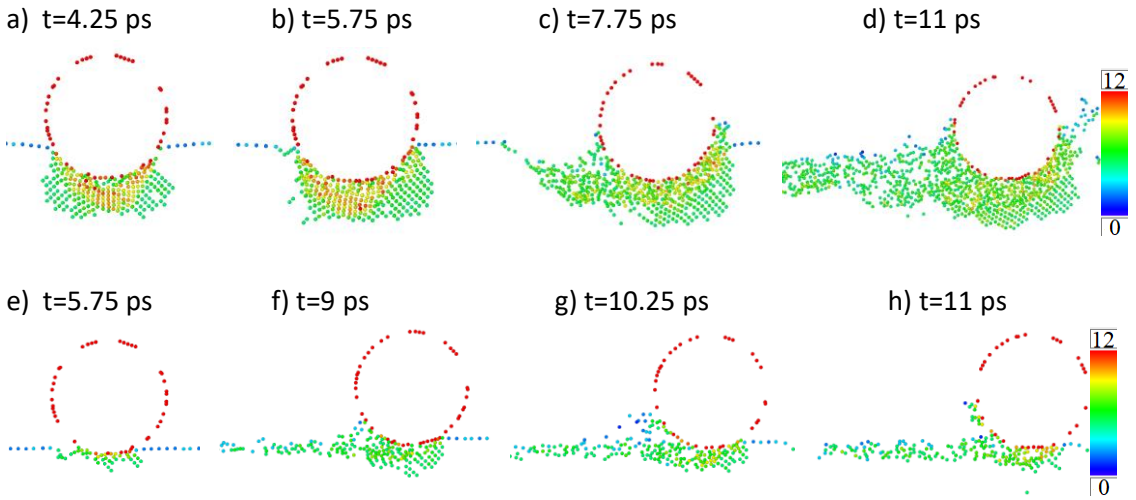

Fig.9: Coordination number of workpiece atoms with different time of polishing. Colour bar indicate coordination number red=12 and dark blue=0. (a-d) with indentation force =757 nN. (e-h) with indentation force =95 nN.

To understand the previous mechanism of surface buckling and the phase transformation, a parametric study is carried out with different levels of indentation forces and the same is presented in following parts of the paper.

An average cohesive energy of Si-workpiece atoms is analysed and presented in *Fig.10* which indicate how the potential energy of Si-atoms varies with polishing time at different level of indentation forces. It is observed that the indentation force increases cohesive energy which means that the amorphous layer formation through indentation force increases potential energy and workpiece becomes chemically unstable. This chemical instability will be helpful to augment the chemical reaction when polishing is carried out through chemo-mechanical polishing, and it will lead to high material removal. During indentation, energy drops after 4 ps as shown in the inset photo of *Fig.10*. This is happening due the transformation of β-Si in to amorphous silicon by the transformation of coordination of CN5 →CN6 as shown in *Fig.8(a)*. Thereafter, it further reduces as seen near 5 ps. In this case, abrasive lateral movement starts which helps to release the compressive stress from the β-Si, and the lattice transformation reaction forms more CN6 atoms trailing to the abrasive as shown in *Fig.8(b)*. Afterwards, energy increases linearly due to swiping of abrasive on workpiece and increases zones of transformed lattices with additional formation of CN2 and CN3.

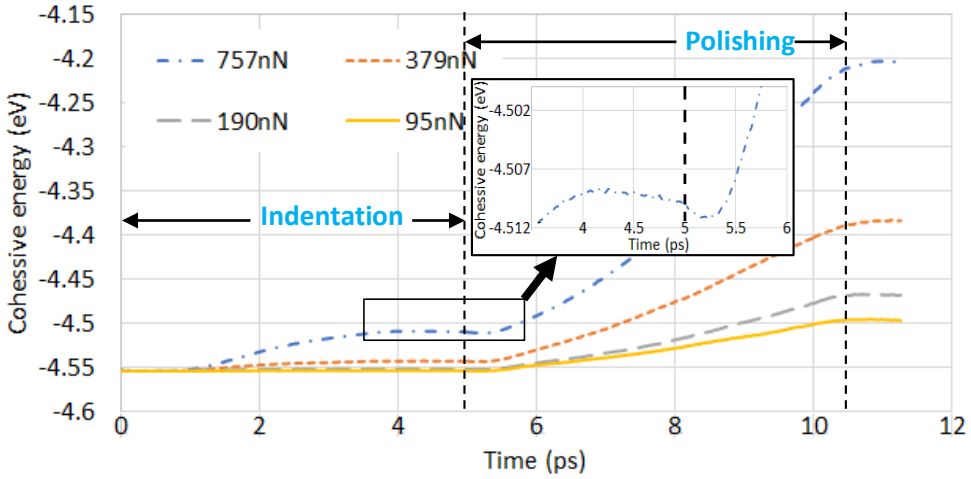

Fig.10: Average cohesive energy of silicon atoms during polishing with different levels (95 nN, 190 nN, 379 nN and 757 nN) of indentation force.

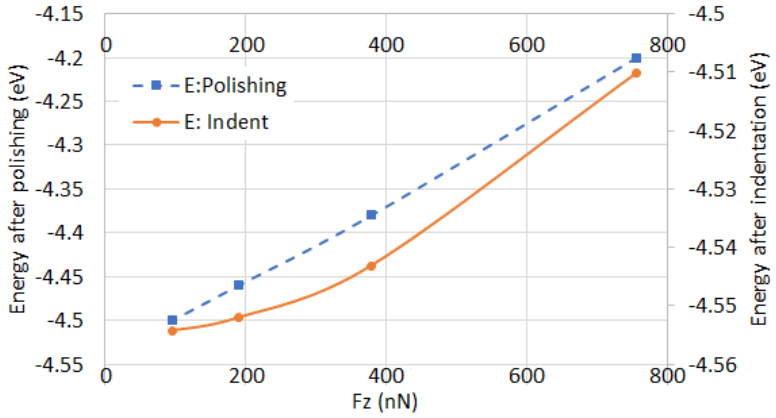

Fig.11: Effect of indentation force (Fz) on indentation as well as polishing on the average cohesive energy of Si-atoms.

Fig.11 is plotted to understand the effect of indentation force on the energy. It is found that the indentation force of 95 nN and 190 nN has less effect on the raise of energy during indentation. Afterwards, it increases rapidly. Based on the geometry, indentation force needs to be linearly proportional to the depth of indentation provided abrasive diameter is more than one order of the indentation depth. However, the stress affected atoms which transforms the lattice structure is not linear with the indentation depth and this might be the reason that small indentation force creating only β-Si as shown in *Fig.9(e)*. Moreover, higher indentation inducing formation CN6 atoms with tensile stress region as shown in *Fig.9(a)* and *Fig.4(c)*. *Fig.11* also shows energy after polishing which increases linearly with respect to the indentation force. This happens due to the mechanism of material removal without surface buckling which compensate the number amorphous atoms at smaller indentation force. It means that the raise in potential energy at smaller indention force leads to efficient material removal and removed atoms indicates raise in the energy. On other hand, higher indentation leads to surface and sub-surface damages of workpiece towards raise in the potential energy.

In order to quantify the damaged surface of workpiece, radial distribution function (RDF) is computed for all levels of indentation force and they are plotted after polishing as shown in *Figs.12(a-b)*. It is noticed that the RDF peak at bond length of 2.35 Å decrease with the force as shown in *Fig.12(a)*, where, 2.35 Å of bond length indicates diamond cubic lattice. This results indicates that the indentation force damages lattice of Si-workpiece linearly. However, in case of smaller force 95 nN and 190 nN, the peak height does not change as shown in *Fig.12(b)* which implies that the smaller force does not affect the lattice of parent material of Si-workpiece and material removal is taking place without surface buckling.

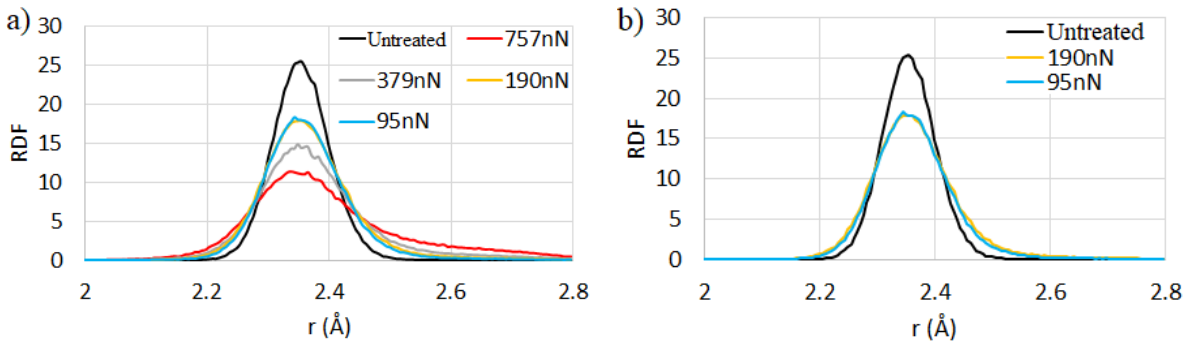

Fig.12: Radial distribution function (RDF) with different level of indentation force. (a) Fz=95 nN, 190 nN, 379 nN and 757 nN. (b) Fz=95 nN and 190 nN.

Conclusions

In this paper, molecular dynamics simulations are carried out to investigate the mechanism of material removal while diamond polishing of monocrystalline silicon with different level of indentation force. The conclusions are summarised as follows.

- Higher amount of indentation force induces compressive stress along lateral direction and a combination of both tensile as well as compressive stresses along indentation direction.
- The atoms in front of abrasive experience tensile stress due to the phenomenon of surface buckling at higher indentation force. This further leads to form a thin squeezed film of Si-atoms ahead of abrasive particle.
- The indentation force with the value of 190 nN or less mitigates the possibility of the surface buckling which helps to mitigate any kinds of residual stress. In this case, material removal is taking place purely in form of rolling followed by adhesion debonding which is favourable for ultra-precision polishing of silicon.
- It is observed that the indentation force increases potential energy of silicon workpiece by the way to form chemically unstable amorphous layer. This chemical instability helps to augment the chemical reaction when polishing is carried out through chemo-mechanical polishing.
- Based on the study, it is essential to polish Si-workpiece in stage wise manner in which indentation force (or polishing pressure in lapping or chemo-mechanical polishing) can be small for the last stage of polishing to minimise the surface defects towards ultra-precision polishing. Whereas, initial stage with higher indentation force is required for

higher material removal to eliminate all defects and residual stress from the workpiece material.

- During diamond lapping of silicon, the lattice transformation happens different in compressive and tensile loading condition. For example, the lattice transformation under compressive stress converts diamond cubic-Si → β-Si → amorphous Si. Whereas, the diamond cubic of Si gets converted in to amorphous Si under tensile stress condition.

In short, polishing of silicon with smaller indention force (less than 190 nN) leads to efficient material removal without affecting lattice structure of workpiece and process the material without surface buckling. On other hand, higher indentation force leads to surface and sub-surface damages of workpiece which is suitable of initial stage of polishing or coarse polishing.

References

[1] D. Zhao, X. Lu, Chemical mechanical polishing: Theory and experiment, Friction. (2013). doi:10.1007/s40544-013-0035-x.

[2] W. Xie, Z. Zhang, S. Yu, L. Li, X. Cui, Q. Gu, Z. Wang, High efficiency chemical mechanical polishing for silicon wafers using a developed slurry, Surfaces and Interfaces. (2023). doi:10.1016/j.surfin.2023.102833.

[3] W. Xie, Z. Zhang, L. Wang, X. Cui, S. Yu, H. Su, S. Wang, Chemical mechanical polishing of silicon wafers using developed uniformly dispersed colloidal silica in slurry, J. Manuf. Process. (2023). doi:10.1016/j.jmapro.2023.01.007.

[4] Z. Liang, Y. Wu, X. Wang, W. Zhao, A new two-dimensional ultrasonic assisted grinding (2D-UAG) method and its fundamental performance in monocrystal silicon machining, Int. J. Mach. Tools Manuf. (2010). doi:10.1016/j.ijmachtools.2010.04.005.

[5] E. Shamoto, T. Moriwaki, Study on Elliptical Vibration Cutting, CIRP Ann. - Manuf. Technol. (1994). doi:10.1016/S0007-8506(07)62158-1.

[6] J.F. Yin, Q. Bai, B. Zhang, Methods for detection of subsurface damage: A review, Chinese J. Mech. Eng. (English Ed. (2018). doi:10.1186/s10033-018-0229-2.

[7] Y. Yan, Z. Li, J. Jia, J. Wang, Y. Geng, Molecular dynamics simulation of the combination effect of the tip inclination and scratching direction on nanomachining of single crystal silicon, Comput. Mater. Sci. (2021). doi:10.1016/j.commatsci.2020.110014.

[8] V.T. Nguyen, T.H. Fang, Molecular dynamics simulation of abrasive characteristics and interfaces in chemical mechanical polishing, Appl. Surf. Sci. (2020). doi:10.1016/j.apsusc.2019.144676.

[9] P. Ranjan, A. Sharma, T. Roy, R. Balasubramaniam, V.K. Jain, Molecular dynamics simulation of mechanical polishing, Int. J. Precis. Technol. 8 (2019) 335. doi:10.1504/ijptech.2019.10022599.

[10] L. Zhang, H. Zhao, Z. Ma, H. Huang, C. Shi, W. Zhang, A study on phase transformation of monocrystalline silicon due to ultra-precision polishing by molecular dynamics simulation, AIP Adv. (2012). doi:10.1063/1.4763462.

[11] B. Zhu, D. Zhao, H. Zhao, J. Guan, P. Hou, S. Wang, L. Qian, A study on the surface quality and brittle-ductile transition during the elliptical vibration-assisted nanocutting process on monocrystalline silicon via molecular dynamic simulations, RSC Adv. (2017). doi:10.1039/C6RA25426H.

[12] H. Dai, G. Chen, S. Li, Q. Fang, B. Hu, Influence of laser nanostructured diamond

tools on the cutting behavior of silicon by molecular dynamics simulation, RSC Adv. (2017). doi:10.1039/c6ra27070k.
[13] H. Dai, F. Zhang, J. Chen, A study of ultraprecision mechanical polishing of single-crystal silicon with laser nano-structured diamond abrasive by molecular dynamics simulation, Int. J. Mech. Sci. (2019). doi:10.1016/j.ijmecsci.2019.04.027.
[14] S.N. Ameli Kalkhoran, M. Vahdati, J. Yan, Effect of relative tool sharpness on subsurface damage and material recovery in nanometric cutting of mono-crystalline silicon: A molecular dynamics approach, Mater. Sci. Semicond. Process. (2020). doi:10.1016/j.mssp.2019.104868.
[15] H. Dai, Y. Zhou, P. Li, Y. Zhang, Evolution of nano-cracks in single-crystal silicon during ultraprecision mechanical polishing, J. Manuf. Process. (2020). doi:10.1016/j.jmapro.2020.08.005.
[16] J. Tersoff, Modeling solid-state chemistry: Interatomic potentials for multicomponent systems, Phys. Rev. B. 39 (1989) 5566–5568. doi:10.1103/PhysRevB.39.5566.
[17] J. Tersoff, Erratum: Modeling solid-state chemistry: Interatomic potentials for multicomponent systems, Phys. Rev. B. (1990). doi:10.1103/PhysRevB.41.3248.2.
[18] S.A. Hollingsworth, R.O. Dror, Molecular Dynamics Simulation for All, Neuron. (2018). doi:10.1016/j.neuron.2018.08.011.
[19] J. Stadler, R. Mikulla, H.R. Trebin, IMD: A software package for molecular dynamics studies on parallel computers, Int. J. Mod. Phys. C. 8 (1997) 1131–1140. http://apps.isiknowledge.com/full_record.do?product=WOS&search_mode=GeneralSearch&qid=51&SID=W1ki6LhmKpGP@h3A2HP&page=1&doc=8.
[20] A. Stukowski, Visualization and analysis of atomistic simulation data with OVITO–the Open Visualization Tool, Model. Simul. Mater. Sci. Eng. 18 (2009) 015012. doi:10.1088/0965-0393/18/1/015012.
[21] A.K. Subramaniyan, C.T. Sun, Continuum interpretation of virial stress in molecular simulations, Int. J. Solids Struct. 45 (2008) 4340–4346. doi:10.1016/j.ijsolstr.2008.03.016.
[22] S. Goel, S.S. Joshi, G. Abdelal, A. Agrawal, Molecular dynamics simulation of nanoindentation of Fe3C and Fe4C, Mater. Sci. Eng. A. 597 (2014) 331–341. doi:10.1016/j.msea.2013.12.091.